Climate and the Collapse of Maya Civilization

Article *in* Science · April 2003

DOI: 10.1126/science.1080444 · Source: PubMed

CITATIONS
593

READS
810

6 authors, including:

Detlef Günther
ETH Zurich
506 PUBLICATIONS **21,176** CITATIONS
SEE PROFILE

Larry C. Peterson
University of Miami
176 PUBLICATIONS **10,316** CITATIONS
SEE PROFILE

Daniel M Sigman
Princeton University
274 PUBLICATIONS **19,938** CITATIONS
SEE PROFILE

Konrad Hughen
Woods Hole Oceanographic Institution
188 PUBLICATIONS **24,853** CITATIONS
SEE PROFILE

the deep ocean, as its mixing time is close to the observed 800-year lag.

Finally, the situation at Termination III differs from the recent anthropogenic CO_2 increase. As recently noted by Kump (*38*), we should distinguish between internal influences (such as the deglacial CO_2 increase) and external influences (such as the anthropogenic CO_2 increase) on the climate system. Although the recent CO_2 increase has clearly been imposed first, as a result of anthropogenic activities, it naturally takes, at Termination III, some time for CO_2 to outgas from the ocean once it starts to react to a climate change that is first felt in the atmosphere. The sequence of events during this Termination is fully consistent with CO_2 participating in the latter ~4200 years of the warming. The radiative forcing due to CO_2 may serve as an amplifier of initial orbital forcing, which is then further amplified by fast atmospheric feedbacks (*39*) that are also at work for the present-day and future climate.

References and Notes

1. J. R. Petit *et al.*, *Nature* **399**, 429 (1999).
2. A. Neftel, H. Oeschger, T. Staffelbach, B. Stauffer, *Nature* **331**, 609 (1988).
3. D. Raynaud *et al.*, *Science* **259**, 926 (1993).
4. J. M. Barnola, D. Raynaud, Y. S. Korotkevich, C. Lorius, *Nature* **329**, 408 (1987).
5. D. M. Sigman, E. A. Boyle, *Nature* **407**, 859 (2000).
6. In 1999, Fischer *et al*. (*30*) estimated that the increase of CO_2 lagged Vostok temperature by 600 ± 400 years at the start of the last three Terminations, but the gas age–ice age difference at Vostok may be uncertain by 1000 years (*1*) and thus obscures the phasing of gas variations with climate signals borne by the ice.
7. The firn is the uppermost part of an ice sheet. It can be schematically divided into three zones with different properties concerning the movement of air: the convective zone in which the air is well mixed, the diffusive zone in which vertical transport is driven by molecular diffusion, and the nondiffusive zone in which air does not migrate vertically, and at the bottom of which the air is trapped (*17*). This entrapped air is younger than the surrounding ice, which results in an age difference (Δage) between the ice and the air bubbles that it contains.
8. T. Blunier *et al.*, *Geophys. Res. Lett.* **24**, 2683 (1997).
9. E. Monnin *et al.*, *Science* **291**, 112 (2001).
10. N. Caillon, J. Jouzel, J. Chappellaz, A. Grachev, unpublished data.
11. C. Lang, M. Leuenberger, J. Schwander, S. Johnsen, *Science* **286**, 934 (1999).
12. M. Leuenberger, C. Lang, J. Schwander, *J. Geophys. Res.* **104**, 22163 (1999).
13. J. P. Severinghaus, T. Sowers, E. Brook, R. Alley, M. Bender, *Nature* **391**, 141 (1998).
14. J. P. Severinghaus, J. Brook, *Science* **286**, 930 (1999).
15. N. Caillon *et al.*, *J. Geophys. Res.* **106**, 31893 (2001).
16. The argon peak around 2760 m has no counterpart in the temperature record published in (*1*). In Fig. 1B, we plotted the temperature profile that we deduced from the new deuterium measurements performed every 10 cm (between 2700 and 2800 m). During the cooling phase of the interglacial, several abrupt temperature fluctuations occurred [especially around 235,000 years (2740 m)], which were not revealed by the temperature profile in (*1*). Those temperature variations could have affected the isotopic composition of argon, making the argon peak at 2760 m. However, the sampling frequency in this depth range (2775 to 2750 m) does not allow access to a $\delta^{40}Ar$ record as precise as that which we obtained during the Termination (i.e., between 2830 and 2775 m) and does not allow a peak-to-peak correlation.
17. T. A. Sowers, M. Bender, D. Raynaud, Y. S. Korotkevich, *J. Geophys. Res.* **97**, 15683 (1992).
18. Dynamic densification firn models accounting for heat transfer are now under development. First results predict that part of the measured argon signal should be a result of thermal diffusion (*40*, *41*). Those models suggest that despite the slow time scale of warming during the Termination, there is still a small residual temperature gradient left over after thousands of years, because of the low thermal conductivity of the firn. The models generate a temperature gradient between surface and close-off region of about 3 K, which leads to a thermal diffusion signal of about 0.11‰ using measured thermal diffusion coefficients (*19, 42*). The use of a precise record of $\delta^{15}N$, which is more sensitive to thermal diffusion than $\delta^{40}Ar/4$, over the Termination should be useful to confirm the small thermal diffusion signal predicted by their models. Indeed, $\delta^{15}N$ data should have a slightly larger value than $\delta^{40}Ar/4$ to be consistent with the presence of thermal diffusion signal (*13*). However, a precise record of $\delta^{15}N$ for Termination III is not available (fig. S1).
19. J. P. Severinghaus, A. Grachev, B. Luz, N. Caillon, *Geochim. Cosmochim. Acta* **67**, 325 (2003).
20. L. Arnaud, J.-M. Barnola, P. Duval, in *Physics of Ice Core Records*, T. Hondoh, Ed. (Hokkaido Univ. Press, Sapporo, Japan, 2000), pp. 285–305.
21. C. Lorius *et al.*, *Nature* **316**, 591 (1985).
22. The deuterium content of the snow in East Antarctica is linearly related to the surface temperature of the precipitation site. Jouzel and colleagues (*43*) have reviewed all relevant information focusing on the East Antarctic Plateau where both model and empirical isotope-temperature estimates are available. Combining arguments coming from the isotopic composition of the air bubbles, from constraints with respect to ice core chronologies, from atmospheric general circulation models, and from isotopic general circulation models (see references herein), the authors suggest that, unlike for Greenland, the present-day spatial isotope-temperature slope can be taken as a surrogate of the temporal slope to interpret glacial-interglacial isotopic changes at sites such as Vostok.
23. O. Watanabe *et al.*, *Nature*, in press.
24. J. P. Severinghaus, A. Grachev, M. Battle, *Geochem. Geophys. Geosyst.* **2**, Paper no. 2000GC000146 (2001).
25. N. Caillon, thesis, University of Paris 6, France (2001).
26. M. Battle *et al.*, *Nature* **383**, 231 (1996).
27. The nondiffusive zone is at the bottom of the firn and thus warms several hundred years after the surface because of the slow diffusion of heat through the firn (*4*). Additionally, the low accumulation rates at Vostok make the downward transport of firn physical properties rather slow (potentially spanning thousands of years). For example, if strong winds during the glacial periods created wind-packed layers that later impeded gas diffusion, thus creating a very thick nondiffusive zone, these layers would take several thousand years to be transported down to the nondiffusive zone.
28. T. Sowers, M. Bender, D. Raynaud, Y. S. Korotkevich, J. Orchado, *Paleoceanography* **6**, 669 (1991).
29. J. Jouzel *et al.*, *Quat. Sci. Rev.* **21**, 307 (2002).
30. H. Fischer, M. Wahlen, J. Smith, D. Mastroianni, B. Deck, *Science* **283**, 1712 (1999).
31. C. Genthon *et al.*, *Nature* **329**, 414 (1987).
32. N. J. Shackleton, *Science* **289**, 1897 (2000).
33. H. J. Smith, H. Fischer, M. Wahlen, D. Mastroianni, B. Deck, *Nature* **400**, 248 (1999).
34. J. R. Toggweiler, *Paleoceanography* **14**, 572 (1999).
35. B. Stephens, R. Keeling, *Nature* **404**, 171 (2000).
36. J. H. Martin, R. M. Gordon, S. E. Fitzwater, *Nature* **345**, 156 (1990).
37. W. S. Broecker, G. M. Henderson, *Paleoceanography* **13**, 352 (1998).
38. L. R. Kump, *Nature* **419**, 188 (2002).
39. C. Lorius, J. Jouzel, D. Raynaud, J. Hansen, H. Le Treut, *Nature* **347**, 139 (1990).
40. J. Schwander, personal communication.
41. C. Goujon, personal communication.
42. A. M. Grachev and J. P. Severinghaus, *Geochim. Cosmochim. Acta* **67**, 345 (2003).
43. J. Jouzel *et al.*, *J. Geophys. Res.*, in press.
44. L. Pépin, D. Raynaud, J.-M. Barnola, M. F. Loutre, *J. Geophys. Res.* **106**, 31885 (2001).

45. We acknowledge the effort of the Russian Antarctic expeditions (RAE), the division of Polar Programs (NSF), and the Institut Polaire Paul Emile Victor (IPEV) for their participation in the Vostok Project. We thank T. Sowers, M. Leuenberger, and J. Schwander for their pertinent and useful reviews; and J. Chappellaz, V. Masson-Delmotte, J.-R. Petit, F. Parrenin, H. Gildor, L. Pépin, M. Bender, R. Keeling, A. Landais, V. Caillon, C. Gougon, and B. Bellier for help and for fruitful comments and discussions. This work was supported by the French Programme National d'Études de la Dynamique du Climat (PNEDC), the CEA, the Balzam Foundation, the European program Pole-Ocean-Pole (POP EVK2-2000-00089), by NSF grants OPP 9725305 and ATM 9905241 (J.P.S.), and by recruitment funds from the Scripps Institution of Oceanography.

Supporting Online Material

www.sciencemag.org/cgi/content/299/5613/1728/DC1
Fig. S1

25 September 2002; accepted 10 February 2003

Climate and the Collapse of Maya Civilization

Gerald H. Haug,[1]*† Detlef Günther,[2] Larry C. Peterson,[3] Daniel M. Sigman,[4] Konrad A. Hughen,[5] Beat Aeschlimann[2]

In the anoxic Cariaco Basin of the southern Caribbean, the bulk titanium content of undisturbed sediment reflects variations in riverine input and the hydrological cycle over northern tropical South America. A seasonally resolved record of titanium shows that the collapse of Maya civilization in the Terminal Classic Period occurred during an extended regional dry period, punctuated by more intense multiyear droughts centered at approximately 810, 860, and 910 A.D. These new data suggest that a century-scale decline in rainfall put a general strain on resources in the region, which was then exacerbated by abrupt drought events, contributing to the social stresses that led to the Maya demise.

Paleoclimatologists have developed an increasingly precise record of climate change for the past few millennia, covering the same span of time over which literate human societies developed. Until recently, archaeologists and historians have lacked information about short-term climate change during the period of human societal evolution, being forced into the assumption that global climate has been nearly invariant for at least the past 6000 years. How-

ever, high-resolution paleoclimate records from ice cores, tree rings, and some deep-sea and lacustrine sediments now make it clear that climatic shifts did occur within the late Holocene and that these often coincided with twists and turns in human history (*1*). Unfortunately, the limitations of temporal resolution and chronology in paleoclimatic records still present a major obstacle to the development of a globally meaningful view of Holocene climatic changes and their role in social change.

Here we report data from annually laminated sediments of the anoxic Cariaco Basin off northern Venezuela (Fig. 1). Using measurements of bulk sediment chemistry, we developed a record of varying river-derived inputs having roughly bimonthly resolution for the period from 700 to 950 A.D., an interval known as the Terminal Classic Period, during which Classic Maya civilization collapsed in the lowlands of the Yucatan Peninsula (Fig. 1). Our data show a clear link between the chronology of regional drought and the demise of Classic Maya culture.

This study focused on the Holocene sediment sequence recovered in Ocean Drilling Program (ODP) holes 1002C and 1002D (10°42.73′N, 65°10.18′W; water depth, 893 m) in the Cariaco Basin (*2*). These rapidly deposited (~30 cm per thousand years) organic-rich sediments are visibly laminated and devoid of preserved benthic faunas, indicating anoxic depositional conditions and no disturbance from burrowing. As an index for regional hydrologic conditions, we used the bulk titanium (Ti) content as a recorder of terrigenous sediment delivery to the Cariaco Basin from the surrounding watersheds (*3*, *4*). Previously reported Ti data (*4*) for the past 2000 years from hole 1002C (Fig. 2, bottom) were obtained at 2-mm measurement intervals (~4 to 5 years) (*5*). Details of the accelerator mass spectrometry ^{14}C-based age model for these data and the conversion to calendar years can be found in (*4*). For this study, we subsequently analyzed a 30-cm slab sample from accompanying hole 1002D at ultrahigh resolution (50-μm measurement spacing) (*5*). Offset scans along the face of the slab indicated that the hole 1002D data were reproducible at the 50-μm level, which is consistent with observations that the laminae are undisturbed. In the interval of hole 1002D from which the 30-cm slab sample was taken, the typical varve (that is, one light-dark laminae pair) is ~0.4 to 0.5 mm thick. Given the 50-μm measurement spacing, each varve is split by about eight analyses, yielding roughly bimonthly resolution and clear resolution of the annual signal. Ti data from this slab sample were readily correlated to the existing Ti data from hole 1002C (Fig. 2).

The connection between rainfall and riverine detrital input is recorded in the laminated nature of Cariaco Basin sediments. Paired annual laminations in the sediments are the result of large changes in rainfall and wind that occur in this region in response to seasonal shifts in the position of the Intertropical Convergence Zone (ITCZ) (Fig. 1) and its associated belt of convective activity (*6*, *7*). Light-colored laminae consist mostly of biogenic components deposited during the dry winter-spring upwelling season, when the ITCZ is located at its southernmost position and trade winds along the Venezuelan coast are strong. In contrast, dark laminae are deposited during the regional rainy season (summer-fall), when the ITCZ migrates to its most northerly position, almost directly over the Cariaco Basin. Dark-colored laminae are rich in terrigenous grains and record higher inputs of Ti and other lithophilic elements. Our interpretation of bulk Ti content as an index of regional hydrologic change, reflecting variations of the mean ITCZ position with time, is supported by comparison of the Holocene Cariaco record (*4*) with independent paleoclimatic data from nearby Lake Valencia (*8*), Haiti (*9*), the Yucatan (*10*), and Lake Titicaca in Peru (*11*).

Ti concentrations in sediments (ODP hole 1002C) deposited over the past 2000 years (Fig. 2, bottom) were lowest between ~500 and 200 years before the present (yr B.P.), indicating dry conditions during the "Little Ice Age" (*4*). Higher Ti concentrations and wet conditions characterized the time interval from 1070 to 850 yr B.P., a portion of the time span often termed the Medieval Warm Period. Before the sharp Ti rise at ~1070 yr B.P. (930 A.D.), sediment Ti concentrations were of intermediate value, with the exception of pronounced minima centered in our

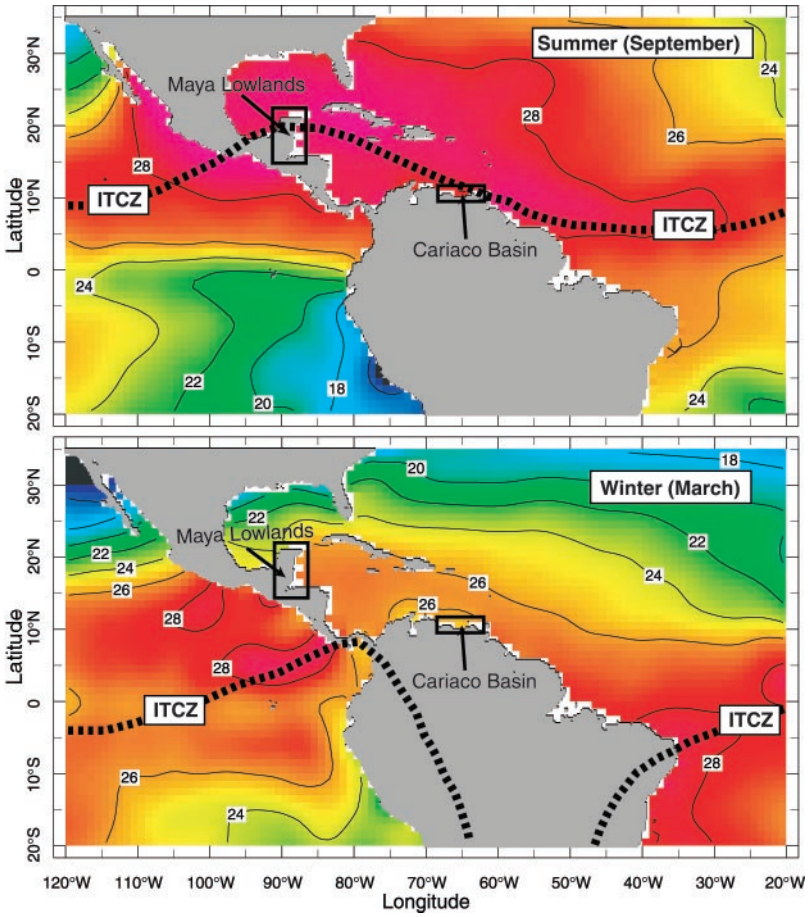

Fig. 1. Seasonal variations in the mean position of the ITCZ over Mesoamerica and northern South America, illustrated for typical summer (September) (**top**) and winter (March) (**bottom**) conditions. These variations control the pattern and timing of regional rainfall. Numbers and colors reflect sea surface temperatures in degrees Celsius. Locations of the Cariaco Basin study area and the Maya lowlands are indicated. Both regions are similarly affected by seasonal and longer term changes in the position of the ITCZ.

[1]Department of Earth Sciences, [2]Department of Chemistry, ETH, CH-8092 Zürich, Switzerland. [3]Rosenstiel School of Marine and Atmospheric Science, University of Miami, Miami, FL 33149, USA. [4]Department of Geosciences, Princeton University, Princeton, NJ 08544, USA. [5]Department of Marine Chemistry and Geochemistry, Woods Hole Oceanographic Institution, Woods Hole, MA 02543, USA.

*To whom correspondence should be addressed. E-mail: haug@gfz-potsdam.de.

†Present address: Geoforschungszentrum Potsdam, D-14473 Potsdam, Germany.

chronology at about 1750 and 1650 yr B.P. and later at 1200 yr B.P. Details of this interval are more clearly visible in our new record from the 30-cm slab sample from ODP hole 1002D (Fig. 2, top). Though highly smoothed (with a 30-point running mean), the ultrahigh-resolution 50-μm measurements from the slab sample faithfully reproduce trends visible in the 2-mm analyses of parallel hole 1002C. Expansion of the upper 9 cm of the 50-μm slab sample data (Fig. 3; three-point running mean) shows a series of four distinct Ti minima at slab depths of ~12, 38, 58, and 78 mm. These are interpreted as evidence for separate multiyear drought events in the region.

It has been suggested that recurrent patterns of drought played an important role in the complex history of the Maya (*10*, *12*, *13*). The Maya civilization developed in a seasonal desert and depended on a consistent rainfall cycle to support agricultural production. Most of the rain falls during the summer, when the ITCZ sits at its northernmost position over the Yucatan (Fig. 1). During the winter, the ITCZ is located south of the lowlands and the climate is dry. Hence, the center of Maya civilization was located in the same climatic regime as the Cariaco Basin, with both areas near the northern limit of seasonal ITCZ motion. An extended southward displacement of the ITCZ, as indicated by low Ti in Cariaco sediments, should lead to similar rainfall reduction in the Maya lowlands.

In order to inhabit the Yucatan lowlands and to deal with normal seasonal variations in rainfall, the Maya developed various strategies to accumulate and store water. Cities were designed to catch the water from rainfall, and quarries and excavations were converted into water reservoirs. The Maya also built on topographic highs to use the hydraulic gradient to distribute the water from canals into complex irrigation systems (*14*, *15*). However, the human-engineered system ultimately depended on seasonal rainfall, because much of the lowlands has only restricted natural groundwater resources.

During the Pre-Classic period before about 150 A.D., Maya culture flourished and the first major cities were built. Between ~150 and 250 A.D., the first documented historical crisis hit the lowlands, which led to the "Pre-Classic abandonment" (*16*) of major cities (Fig. 2). However, populations recovered, cities were reoccupied, and Maya culture blossomed in the following centuries during the so-called Classic period. At the peak of the Classic, around 750 A.D., population estimates for the Maya lowlands range from 3 million to 13 million inhabitants (*17*, *18*).

Between about 750 and 950 A.D., the Maya experienced a demographic disaster as profound as any other in human history. During the Terminal Classic Collapse, many of the densely populated urban centers were abandoned permanently, and Classic Maya civilization came to an end. What happened? Although the Cariaco record cannot provide a complete explanation, it supports the view that changes in rainfall played a critical role. We suggest that the rapid expansion of Maya civilization from 550 to 750 A.D. during climatically favorable (relatively wet) times resulted in a population operating at the limits of the environment's carrying capacity, leaving Maya society especially vulnerable to multiyear droughts. Earlier paleoclimate records from nearby lakes have provided compelling evidence that climate change and aridity played a key role in the collapse of

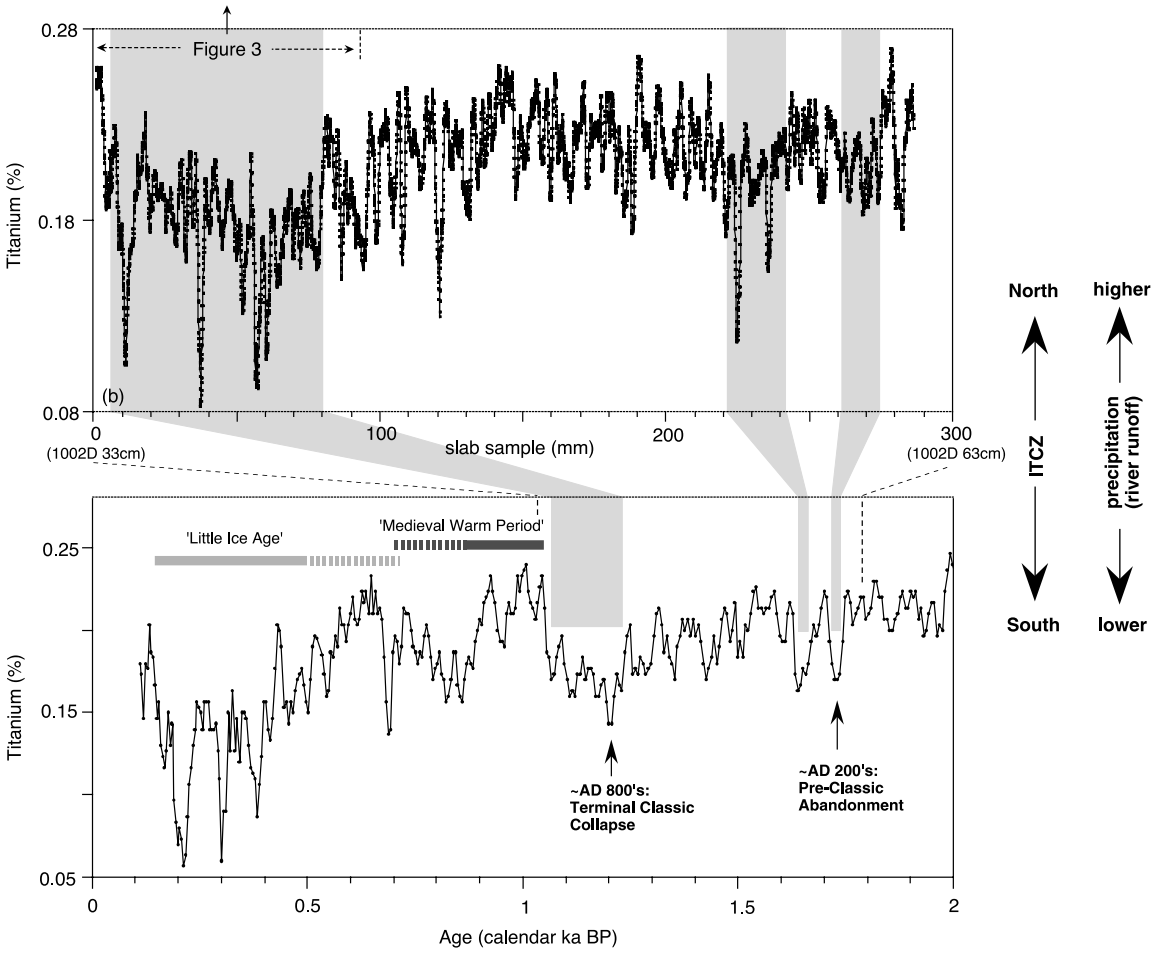

Fig. 2. (**Bottom**) Bulk Ti content [three-point running mean of 2-mm resolution measurements (*4*)] at ODP hole 1002C in the Cariaco Basin during the past 2000 years. The timing of well-known climate events (such as the Little Ice Age) and major events in the history of Maya civilization are shown. The Pre-Classic abandonment and the Terminal Classic Collapse of Maya culture coincided with phases of low riverine-derived Ti input to the Cariaco Basin and with inferred dry conditions in the region. (**Top**) The bulk Ti content (30-point running mean of 50-μm resolution analyses) of a 30-cm-long slab sample from companion ODP hole 1002D in the time interval from about 1.8 to 1.0 thousand years ago confirms these trends and shows increased detail. Periods of drought, marked by low Ti values in the sediments, are likely the result of climatic conditions that prevented the ITCZ and its associated rainfall from penetrating as far north as normal.

Maya culture (*10*, *13*). However, the time resolution of these records has to date been insufficient to provide a precise test of the chronological relationships between climate and cultural changes, despite clear evidence that both occurred. The Cariaco record provides a starting point for integrating these changes into a common history.

Archaeological studies of Maya sites have led to substantial debate over the timing and regional patterning of the Terminal Classic collapse (*16*). Indeed, regional diversity in the timing of cultural transformations during the Terminal Classic period has been used as one argument against drought as a causal factor. The evidence from the Cariaco Basin for a number of distinct multiyear droughts, superimposed on an already generally dry period, may help explain why the so-called collapse was drawn out in time and was regionally variable.

The radiocarbon age control for hole 1002C (*4*) is sufficient to constrain the broad low Ti interval highlighted in Fig. 2 as centered in the 9th century A.D. A tight match with the independently dated megadrought event in the Lake Chichancanab sediment record (*10*, *13*) gives confidence in this absolute age assignment. Taking a date of 930 A.D. for the sharp Ti rise that marks the start of Medieval Warm conditions, the counting of seasonal Ti minima can be used to assign ages to the events below. By this scheme, the distinct Ti minima at depths of ~12, 38, 58, and 78 mm in the hole 1002D slab sample (Fig. 3) mark multiyear drought events that began at about 910, 860, 810, and 760 A.D., respectively. Not counting the duration of the droughts, the number of varves between drought events indicates a spacing of approximately 40 to 47 years (±5), a number that agrees well with observations of subpeaks in the Lake Chichancanab sediment density record at about 50-year intervals (*13*).

Dry conditions beginning about 760 A.D. are clearly marked in the Cariaco Ti record by two large inferred rainfall minima (Fig. 3). Over the subsequent ~40 years, there appears to have been a slight long-term drying trend. This culminated in roughly a decade of more intense aridity that, within the limits of the present chronology, began at about 810 A.D. Drought at about 860 A.D. is recorded by a distinct interval of minimum Ti concentrations, indicating a short (~3 years) but apparently severe event at that time. Finally, low Ti contents in the Cariaco Basin sequence indicate the onset of yet another drought at about 910 A.D., this one estimated to have lasted for ~6 years.

Mayanists generally agree that there is strong evidence for regional variability in the Terminal Classic collapse in the archaeological record (*16*). Most would also concur that the collapse occurred first in the southern and central Yucatan lowlands, and that many areas of the northern lowlands underwent a similar decline a century or so later. A more controversial tripartite pattern of city abandonment (*12*), based on analysis of the last dates carved into local monuments (stelae), has been proposed, which calls for separate phases of collapse that terminated respectively at about 810, 860, and 910 A.D. Noting a similarity between these end dates and the timing of especially severe cold spells indicated in Swedish tree ring records (*19*), Gill (*12*) speculated that periods of coincident drought in Mesoamerica led to the Maya demise. There is considerable debate about using the last entries on stone monuments as an accurate record of city abandonment, and only larger (rank order 10 or greater) Maya sites were considered in the analysis of (*12*). Nevertheless, within the uncertainty of our age model, the proposed end dates match the three most severe drought events inferred from the Cariaco Basin record.

Considerable variability exists in the distribution and quality of natural water sources in the Yucatan lowlands (*12*), a factor that would surely come into play during periods of drought. Although the northern lowlands are characterized by the lowest amounts of annual average rainfall, collapsed cenotes in this region provide direct access to the relatively shallow groundwater table. In the central lowlands, some fresh water is available in and around the Petén Lake district. Towards the west and south, however, access to groundwater is scarce, and rainfall was the primary source of water for Maya cities. During sustained drought, access to groundwater was likely an important factor in determining which large population centers could survive.

The control of artificial water reservoirs by Maya rulers may also have played a role in both the florescence and the collapse of Maya civilization. Noting that the scale of artificial water control seems to correlate with the degree of political power of Maya cities, it has been suggested (*20*) that drought may have undermined the institution of Maya rulership when existing ceremonies and technologies failed to provide sufficient water. In this view, the larger regional centers suffered most, whereas secondary and minor Maya population centers that were less dependent on artificial reservoirs and water control were less affected.

No one archaeological model is likely to capture completely a phenomenon as complex as the Maya decline. Nevertheless, the Cariaco Basin sediment record provides support for the hypothesis that regional drought played an important role in the collapse of Classic Maya civilization, and it provides a temporal template against which archaeological data can be compared. Drought conditions may also have been

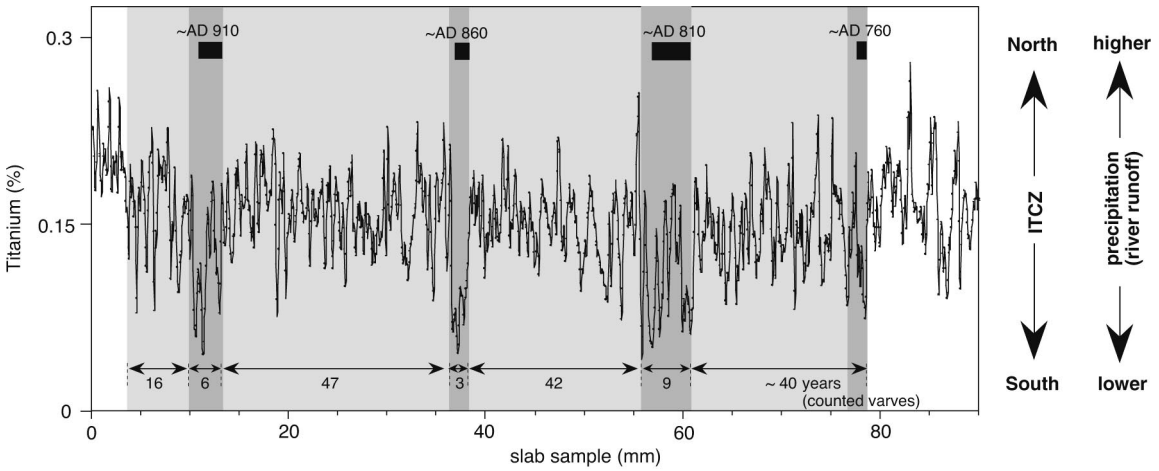

Fig. 3. Bulk Ti content (three-point running mean of 50-μm resolution analyses) centered on the time interval of the collapse of Maya civilization in the Terminal Classic Period. This figure represents an expanded view of the 90-mm slab sample section highlighted in Fig. 2, top. The assignment of ages for prominent drought events (Ti minima) is based on a date of 930 A.D. for the sharp rise in Ti (Fig. 2) that marks the local onset of Medieval Warm conditions, and on varve counting below and throughout this interval. The ability to resolve individual years based on seasonal Ti variations allows for precise estimation of the duration of drought events and of the time between them, although the absolute age of the floating time window is less certain because of the dependence on radiocarbon control with larger errors (±30 years). Evidence presented here for separate and more severe multiyear drought events superimposed on an extended period of overall reduced precipitation may help to explain the multiple stages and regional variability of the Maya collapse.

responsible for the earlier Pre-Classic abandonment of cities that occurred between about 150 and 250 A.D. These periods of drought are probably the result of climatic conditions that prevented the ITCZ and its associated rainfall from penetrating as far north as normal. Given the perspective of our long time series, it would appear that the droughts we have highlighted were the most severe to affect this region in the first millennium A.D. The intervals of peak drought were brief, each lasting between ~3 and 9 years, but they occurred during an extended period of reduced overall precipitation that may have already pushed the Maya system to the verge of collapse.

References and Notes

1. P. B. deMenocal, *Science* **292**, 667 (2001).
2. H. Sigurdsson *et al.*, *Proc. ODP Init. Rep.* **165**, 359 (1997).
3. L. C. Peterson, G. H. Haug, K. A. Hughen, U. Röhl, *Science* **290**, 1947 (2000).
4. G. H. Haug, K. A. Hughen, D. M. Sigman, L. C. Peterson, U. Röhl, *Science* **293**, 1304 (2001).
5. Analyses for the Holocene section at 2 mm resolution were obtained with a profiling x-ray fluorescence scanner at the University of Bremen (*4*). The Ti element mapping at 50 μm resolution was carried out with a Röntgenanalytik Eagle II Micro X-Ray Fluorescence system at ETH Zürich (with the use of an Rh tube at 40 kV and 800 mA). The sediment slab samples from hole 1002D were measured in two parallel and overlapping line scans (sample length, 15 cm). For optimum counting, a measurement time of 24 hours for each sample slab was applied.
6. L. C. Peterson, J. T. Overpeck, N. G. Kipp, J. Imbrie, *Paleoceanography* **6**, 99 (1991).
7. K. A. Hughen, J. T. Overpeck, L. C. Peterson, R. F. Anderson, *Geol. Soc. Spec. Pub.* **116**, 171 (1996).
8. J. P. Bradbury *et al.*, *Science* **214**, 1299 (1981).
9. D. A. Hodell *et al.*, *Nature* **352**, 790 (1991).
10. D. A. Hodell, J. H. Curtis, M. Brenner, *Nature* **375**, 391 (1995).
11. P. A. Baker *et al.*, *Science* **291**, 640 (2001).
12. R. B. Gill, *The Great Maya Droughts: Water, Life and Death* (Univ. of New Mexico Press, Albuquerque, NM, 2000).
13. D. A. Hodell, M. Brenner, J. H. Curtis, T. Guilderson, *Science* **292**, 1367 (2001).
14. R. E. W. Adams, *Science* **251**, 632 (1991).
15. V. L. Scarborough, *Natl. Geogr. Res. Explor.* **10**, 184 (1994).
16. D. Webster, *The Fall of the Ancient Maya* (Thames and Hudson, London, 2002).
17. T. P. Culbert, D. S. Rice, *Precolumbian Population History in the Maya Lowlands* (Univ. of New Mexico Press, Albuquerque, NM, 1990).
18. R. Sharer, *The Ancient Maya* (Stanford Univ. Press, Stanford, CA, 1994).
19. W. Karlén, *Climatic Changes on a Yearly to Millennia Basis: Geological, Historical and Instrumental Records* (Reidel, Dordrecht, Netherlands, 1984).
20. L. J. Lucero, *Am. Anthropol.* **104**, 814 (2002).

21. We thank D. Hodell, J. Bollmann, B. Fagan, C. Rooth, K. Broad, H. Thierstein, and an anonymous referee for helpful discussions and critical comments. This research used samples provided by the Ocean Drilling Program (ODP). The ODP is sponsored by NSF and participating countries under the management of Joint Oceanographic Institutions (JOI). Supported by the Schweizer Nationalfonds and NSF, and by British Petroleum and the Ford Motor Company to D.M.S. through the Princeton Carbon Mitigation Initiative.

13 November 2002; accepted 28 January 2003

Evolution of Virulence in a Plant Host-Pathogen Metapopulation

Peter H. Thrall* and Jeremy J. Burdon

In a wild plant–pathogen system, host resistance and pathogen virulence varied markedly among local populations. Broadly virulent pathogens occurred more frequently in highly resistant host populations, whereas avirulent pathogens dominated susceptible populations. Experimental inoculations indicated a negative trade-off between spore production and virulence. The nonrandom spatial distribution of pathogens, maintained through time despite high pathogen mobility, implies that selection favors virulent strains of *Melampsora lini* in resistant *Linum marginale* populations and avirulent strains in susceptible populations. These results are consistent with gene-for-gene models of host-pathogen coevolution that require trade-offs to prevent pathogen virulence increasing until host resistance becomes selectively neutral.

Infectious disease has a major influence on the demography of human, plant, and animal populations. It is generally accepted that variation in host resistance is of central importance to patterns of disease incidence and prevalence (*1*). High variability has been reported for several host loci (e.g., major histocompatibility complex and/or human leukocyte antigens) linked to disease (*1*, *2*), consistent with the selective forces imposed by pathogens (*3*). At the population level, there are indications that pathogen diversity can determine the dynamics of epidemics (e.g., the slow spread of HIV in some regions may be linked to low genetic variation in particular viral groups) (*4*). Some work has revealed negative relationships between general measures of host diversity and disease incidence (*5*–*7*). More specifically, work on the genetically well-studied *Linum-Melampsora* plant-pathogen system has shown negative correlations between population resistance diversity and disease prevalence (*8*). However, with a few notable exceptions (*9*, *10*), remarkably little effort has been directed at investigating causal links between host population genetic structure and disease dynamics. This is particularly surprising, given the potential for such variation to affect pathogen evolution and the emergence of new diseases (*11*, *12*).

Most mathematical models of the dynamics of host-pathogen coevolution, and indeed much of our current thinking about genetic interactions between hosts and parasites, have been shaped by the gene-for-gene paradigm. Essentially, this hypothesis states that for each host resistance gene, there is a corresponding avirulence gene in the pathogen with which it interacts. For a resistant reaction to occur (i.e., infection does not take place, as the host recognizes the presence of the pathogen), both the specific resistance gene in the host and the avirulence gene in the pathogen must be present. In this context, virulence is defined as the ability of a pathogen to overcome a given host resistance gene. At the population level, virulence can be thought of as the average ability of a pathogen population to overcome the diversity of resistance genes present in the corresponding host population. The gene-for-gene concept is derived from work on cultivated flax and an associated rust pathogen (*13*) but has since been shown to occur in many other systems involving interactions of plants with fungi, viruses, and some insects (*14*).

One such wild gene-for-gene interaction occurs between *L. marginale*, an herbaceous perennial endemic to southern Australia, and its host-specific rust pathogen, *M. lini*. To date, 17 separate alleles conferring resistance to a wide range of pathogen isolates have been detected in this interaction (*15*). During the growing season, generations of the pathogen follow one another in quick succession, leading to local epidemics. On the Kiandra Plain, the phenology of the host results in distinct crashes in pathogen numbers as plants die back to underground rootstocks at the end of the summer.

M. lini is an aerially dispersed rust pathogen that produces large numbers of urediospores that, like most other rust pathogens, may be dispersed large distances. For example, the appearance of a novel pathotype (distinguished by pathogenic and molecular markers) in the Kiandra area is believed to have resulted from a migration event of >100 km (*16*). In field experiments assessing pathogen extinction and recolonization in small populations of *L.*

Commonwealth Scientific and Industrial Research Organization (CSIRO)—Plant Industry, Centre for Plant Biodiversity Research, General Post Office Box 1600, Canberra, ACT 2601, Australia.

*To whom correspondence should be addressed. E-mail: Peter.Thrall@csiro.au